Electronic Supplementary Material (SZI) for Material Advances

Supporting Information

Reassembly of wood to plastic- and paper-like films via ultra-mild dissolution in formic acid

Naoko Kobayashi*[a,f], Tomohiro Hashizume[b,f], Keiko Kondo[c,d,f] Kenji Kitayama[b], Masato Katahira[c,d,e,f] and Takashi Watanabe*[a,f]

Dr. N. Kobayashi* (Kobayashi.naoko.2c@kyoto-u.ac.jp), Prof. T. Watanabe* (twatanab@rish.kyoto-u.ac.jp): Corresponding authors

[a] Biomass Conversion, Research Institute for Sustainable Humanosphere (RISH), Kyoto University, Gokasho, Uji, 611-0011, Japan.

[b] Daicel Corporation, Osaka Head Office, Grand Front Osaka Tower-B, 3-1, Ofuka-cho, Kita-ku, Osaka 530-0011, Japan.

[c] Institute of Advanced Energy, Kyoto University, Gokasho, Uji, Kyoto 611-0011, Japan.

[d] Integrated Research Centre for Carbon Negative Science, Institute of Advanced Energy, Kyoto University, Gokasho, Uji, Kyoto 611-0011, Japan.

[e] Graduate School of Energy Science, Kyoto University, Yoshida-hommachi, Sakyo-ku, Kyoto 606-8501, Japan.

[f] Biomass Product Tree Industry-Academia Collaborative Research Laboratory, Kyoto University, Gokasho, Uji, Kyoto 611-0011, Japan.

Table S1: Comparison of density, maximal stress and strain, Young's, storage (E`), and elastic (E``) moduli, and loss tangent (tanδ) of films from Eucalyptus, Japanese cedar sapwood and heartwood under dissolving temperatures of 30 ℃ to 50 ℃. Table 1 with standard daviations. Five replicates were measured.

Wood powder	Temperature (℃)	Density (g/cm³)	Stress (MPa)	Strain (%)	Young`s modulus (MPa)	E`	E``	tand
						(Tg /℃)		
Eucalyptus	30.0	0.37 ±0.004	3.09 ±0.20	1.16 ±0.11	334.75 ±31.26	230	143	n.d.
	40.0	0.56 ±0.003	31.15 ±4.75	2.73 ±0.62	1745.84 ±105.48	239	243	n.d.
	50.0	0.66 ±0.004	60.98 ±1.92	3.21 ±0.58	3096.73 ±346.81	118	175	177
Japanese cedar (sapwood)	30.0	0.54 ±0.002	2.17 ±0.48	1.19 ±0.06	209.93 ±5.81	245	265	n.d.
	40.0	0.52 ±0.003	10.61 ±1.35	1.94 ±0.15	685.74 ±47.95	251	n.d.	n.d.
	50.0	0.65 ±0.004	5.49 ±0.17	1.35 ±0.07	475.71 ±46.92	261	118	n.d.
Japanese cedar (heartwood)	30.0	0.23 ±0.02	0.59 ±0.16	1.10 ±0.10	n.d.	n.d.	n.d.	n.d.
	40.0	0.50 ±0.008	6.10 ±0.66	1.68 ±0.13	453.45 ±48.53	269	124	n.d.
	50.0	0.64 ±0.004	7.15 ±1.62	1.41 ±0.23	614.81 ±141.63	276	114	n.d.

Table S2: Comparison of density, maximal stress and strain, Young's, storage (E`), and elastic (E``) moduli, and loss tangent (tanδ) of the films from Japanese beech, wheat bran, and sugarcane bagasse under dissolving temperatures at 50 ℃. Table 2 with standard daviations. Five replicates were measured.

Wood powder	Density (g/cm^3)	Stress (MPa)	Strain (%)	Young`s modulus (MPa)	E`	E``	tand
					(Tg /℃)		
Japanese beech	0.90 ±0.005	44.0 ±11.91	2.6 ±0.22	2395.8 ±222.51	141	206	248
Wheat bran	0.44 ±0.002	28.3 ±2.04	3.34 ±0.25	1276.8 ±59.88	109	136	171
Sugarcane bagasse	0.82 ±0.001	60.4 ±3.21	3.27 ±0.20	3592.6 ±102.20	123	155	177

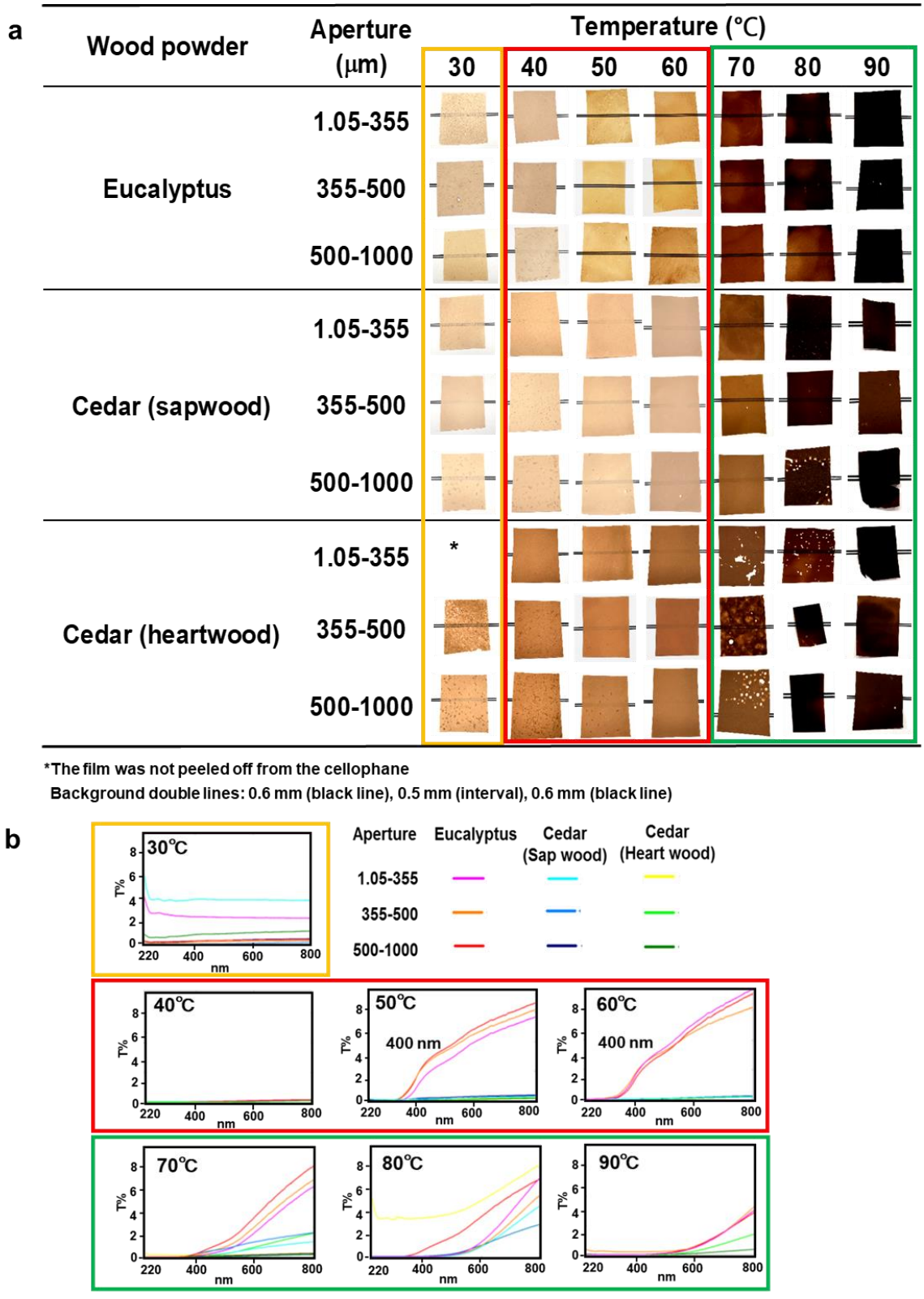

Figure S1: Biomass films and their transmittance spectra prepared from the sawdust of Eucalyptus and Japanese cedar at different dissolving temperatures. a) Biomass films prepared by dissolution of sawdust from Eucalyptus and sapwood and heartwood of Japanese cedar with three different particle sizes (1.05–355, 355–500, and 500–1000 μm) at 30 ℃–90 ℃. The

films were categorized into (1) lump-containing sheet from limited solubilization at 30 ℃ (yellow box); (2) transparent or opaque films prepared at 40 ℃–60 ℃ (red box); and (3) black and fragile films prepared at 70 ℃–90 ℃ (green box). **b,** Transmittance spectra between 220 and 800 nm of the films. Transmittance is summarized in Table S3.

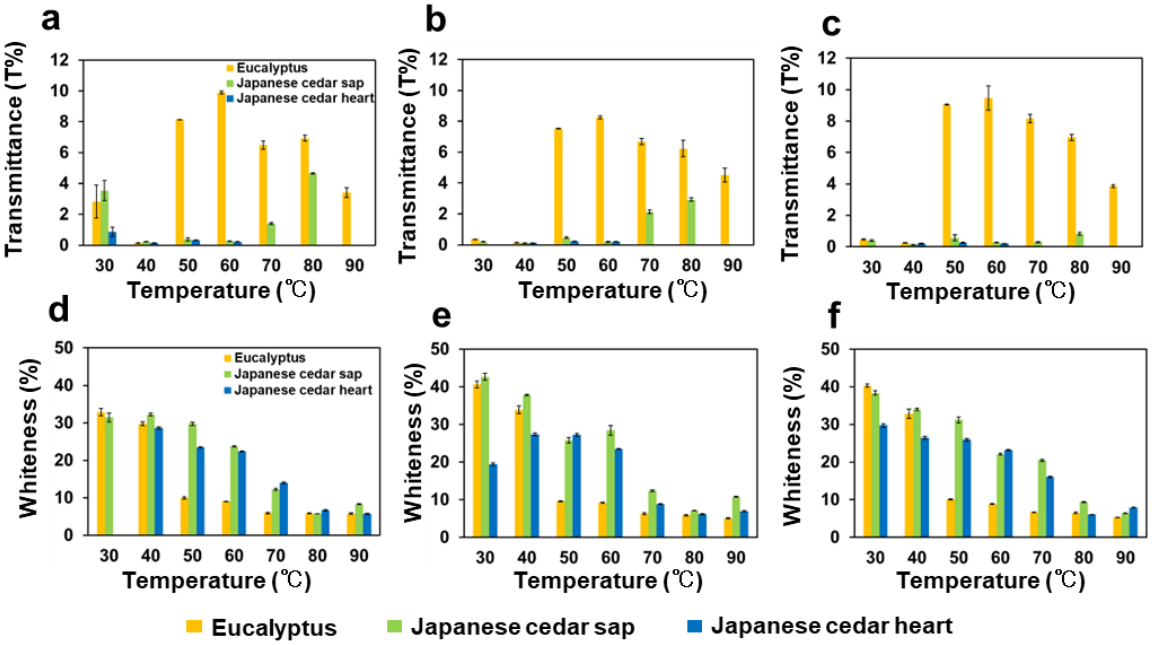

Figure S2: Correlation between transmittance and whiteness of the biomass films from Eucalyptus and Japanese cedar prepared by dissolution at different temperatures. The films were prepared from different sizes of sawdust, 1.05–355 μm (a, d), 355–500 μm (b, e), and 500–1000 μm (c, f), from Eucalyptus (yellow), Japanese cedar sapwood (pale green) and heartwood (blue) at dissolving temperatures of 30 ℃–90 ℃. (a, b, c) All transmittance degrees were measured at 800 nm (Table S3). (d, e, f) Whiteness levels of the films. Whiteness is summarized in Table S4. Five points on the film were measured and calculated for the averages.

Table S3: Transmittance of the films formed from Eucalyptus and sapwood and heartwood of Japanese cedar by dissolution at 30 ℃–90 ℃. Five points on the film were measured and calculated for the averages.

Temperature (℃)	Eucalyptus (T%)			Japanese cedar sap (T%)			Japanese cedar heart (T%)		
	size (mm)			size (mm)			size (mm)		
	1.05-355	355-500	500-1000	1.05-355	355-500	500-1000	1.05-355	355-500	500-1000
30	2.82 ± 1.07	0.36 ± 0.02	0.46 ± 0.03	3.54 ± 0.66	0.19 ± 0.01	0.39 ± 0.05	0.87 ± 0.30	*	*
40	0.15 ± 0.00	0.15 ± 0.00	0.24 ± 0.02	0.21 ± 0.01	0.13 ± 0.00	0.14 ± 0.00	0.14 ± 0.01	0.13 ± 0.01	0.20 ± 0.02
50	8.14 ± 0.00	7.53 ± 0.00	9.05 ± 0.02	0.38 ± 0.11	0.45 ± 0.04	0.57 ± 0.19	0.34 ± 0.01	0.22 ± 0.00	0.26 ± 0.02
60	9.90 ± 0.08	8.25 ± 0.11	9.47 ± 0.78	0.26 ± 0.00	0.18 ± 0.03	0.29 ± 0.01	0.23 ± 0.00	0.21 ± 0.02	0.20 ± 0.01
70	6.48 ± 0.26	6.67 ± 0.19	8.16 ± 0.27	1.40 ± 0.05	2.13 ± 0.11	0.30 ± 0.03	*	*	*
80	6.94 ± 0.20	6.23 ± 0.53	6.96 ± 0.19	4.66 ± 0.04	2.92 ± 0.10	0.82 ± 0.10	*	*	*
90	3.42 ± 0.31	4.51 ± 0.45	3.85 ± 0.08	*	*	*	*	*	*

***Not detected**

Table S4. Whiteness of the films formed from Eucalyptus and sapwood and heartwood of Japanese cedar by dissolving at 30 ℃–90 ℃. Five points on the film were measured and calculated for the averages.

Temperature (℃)	Eucalyptus (T%)			Japanese cedar sap (T%)			Japanese cedar heart (T%)		
	size (mm)			size (mm)			size (mm)		
	1.05-355	355-500	500-1000	1.05-355	355-500	500-1000	1.05-355	355-500	500-1000
30	32.84 ± 0.95	40.62 ± 0.94	40.32 ± 0.45	31.44 ± 1.17	42.66 ± 0.88	38.36 ± 0.56	*	19.42 ± 0.34	29.74 ± 0.42
40	29.82 ± 0.50	33.88 ± 1.08	32.86 ± 1.21	32.28 ± 0.38	37.82 ± 0.20	34.02 ± 0.31	28.60 ± 0.26	27.40 ± 0.37	26.44 ± 0.36
50	10.02 ± 0.32	9.58 ± 0.13	10.12 ± 0.11	29.72 ± 0.43	25.76 ± 0.75	31.18 ± 0.75	23.46 ± 0.13	27.22 ± 0.38	25.94 ± 0.26
60	9.00 ± 0.07	9.22 ± 0.15	8.90 ± 0.16	23.72 ± 0.11	28.42 ± 1.29	22.04 ± 0.23	22.36 ± 0.16	23.44 ± 0.11	23.20 ± 0.10
70	5.94 ± 0.17	6.26 ± 0.23	6.66 ± 0.09	12.28 ± 0.25	12.36 ± 0.21	20.46 ± 0.32	13.96 ± 0.26	8.80 ± 0.12	16.04 ± 0.22
80	5.86 ± 0.09	5.90 ± 0.19	6.50 ± 0.23	5.70 ± 0.00	7.14 ± 0.05	9.36 ± 0.11	6.66 ± 0.21	6.18 ± 0.11	6.08 ± 0.04
90	5.78 ± 0.16	5.02 ± 0.13	5.32 ± 0.08	8.34 ± 0.15	10.78 ± 0.08	6.40 ± 0.07	5.72 ± 0.11	6.94 ± 0.15	7.96 ± 0.05

*Not detected

Table S5. Comparison of transmittance and whiteness of the films formed for different species, tissues, and sources by dissolving at 30 ℃–90 ℃. Five points on the film were cmeasured and alculated for the averages.

Materials	Transmittance (T%)	Whiteness (%)
Japanese cedar (sapwood)	**0.21 ± 0.01**	**36.84 ± 1.62**
Japanese cedar (heartwood)	**0.29 ± 0.06**	**27.00 ± 0.56**
Rice fir	**0.34 ± 0.01**	**40.14 ± 0.85**
Japanese beech	**6.70 ± 0.85**	**7.54 ± 0.39**
Japanese cypress	**5.88 ± 0.25**	**7.90 ± 0.35**
Japanese red pine	**8.02 ± 0.66**	**8.56 ± 0.18**
Sugarcane baggase	**5.98 ± 0.12**	**9.40 ± 0.12**
Bomboo	**6.11 ± 0.60**	**9.30 ± 0.37**
Wheat bran	**16.09 ± 0.88**	**8.96 ± 0.06**

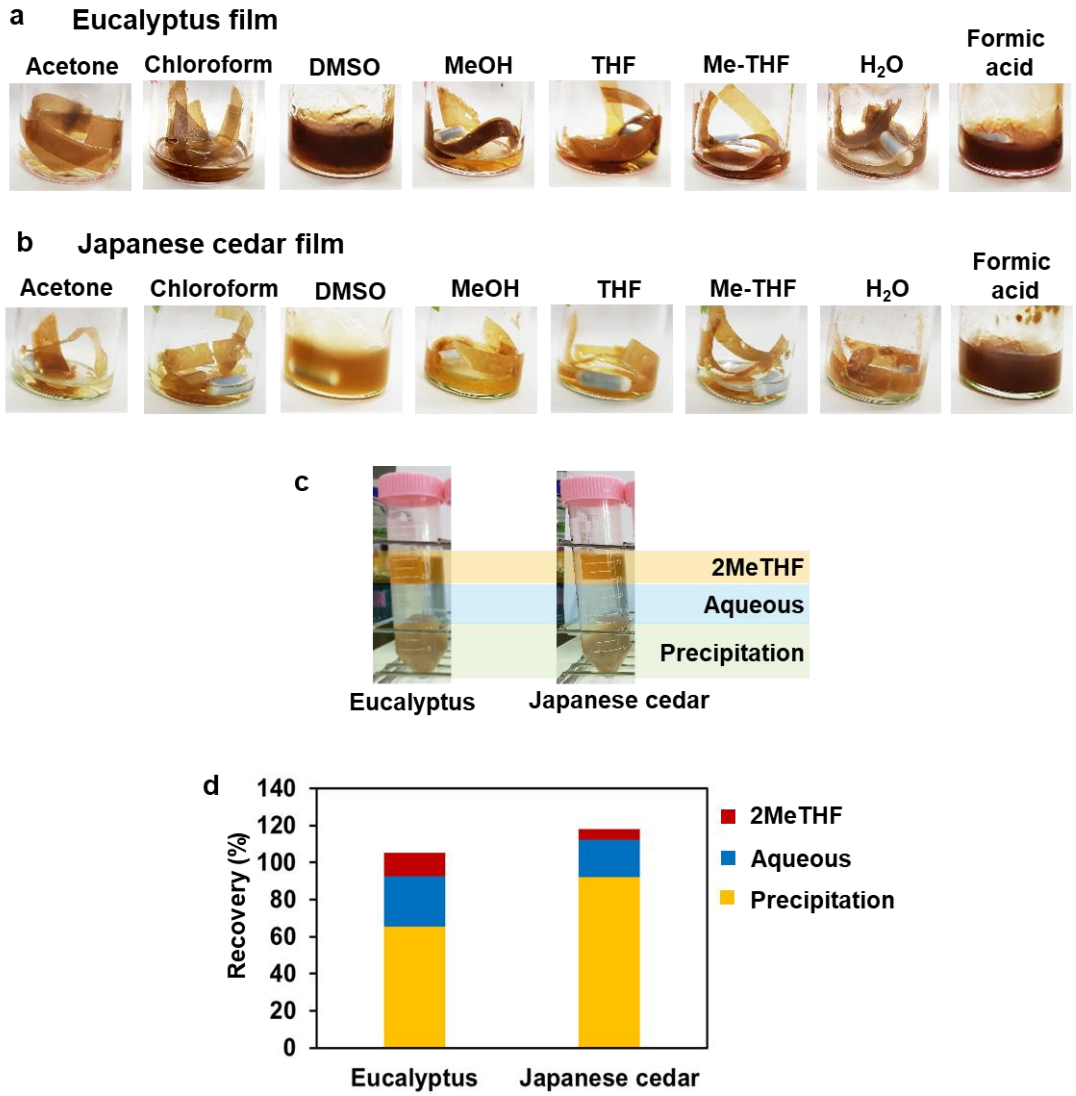

Figure S3: Comparison of soulubilization in different solvent and fractionation of biomass films by phase separation. Solubilazation of Eucaluptus (a) and Japanese cedar (b) biomass film in different solvent. Biomass film was stirred in each solvent for overnight at 40 ℃. (c) Biomass films were prepared by dissolution of Eucalyptus and Japanese cedar heartwood at 50 ℃. The films were redissolved in formic acid and separated by phase-partition with 2MeTHF and water. Each fraction was analyzed by NMR spectroscopy. (d) Recoveries of the three fractions from Eucalyptus and Japanese cedar films.

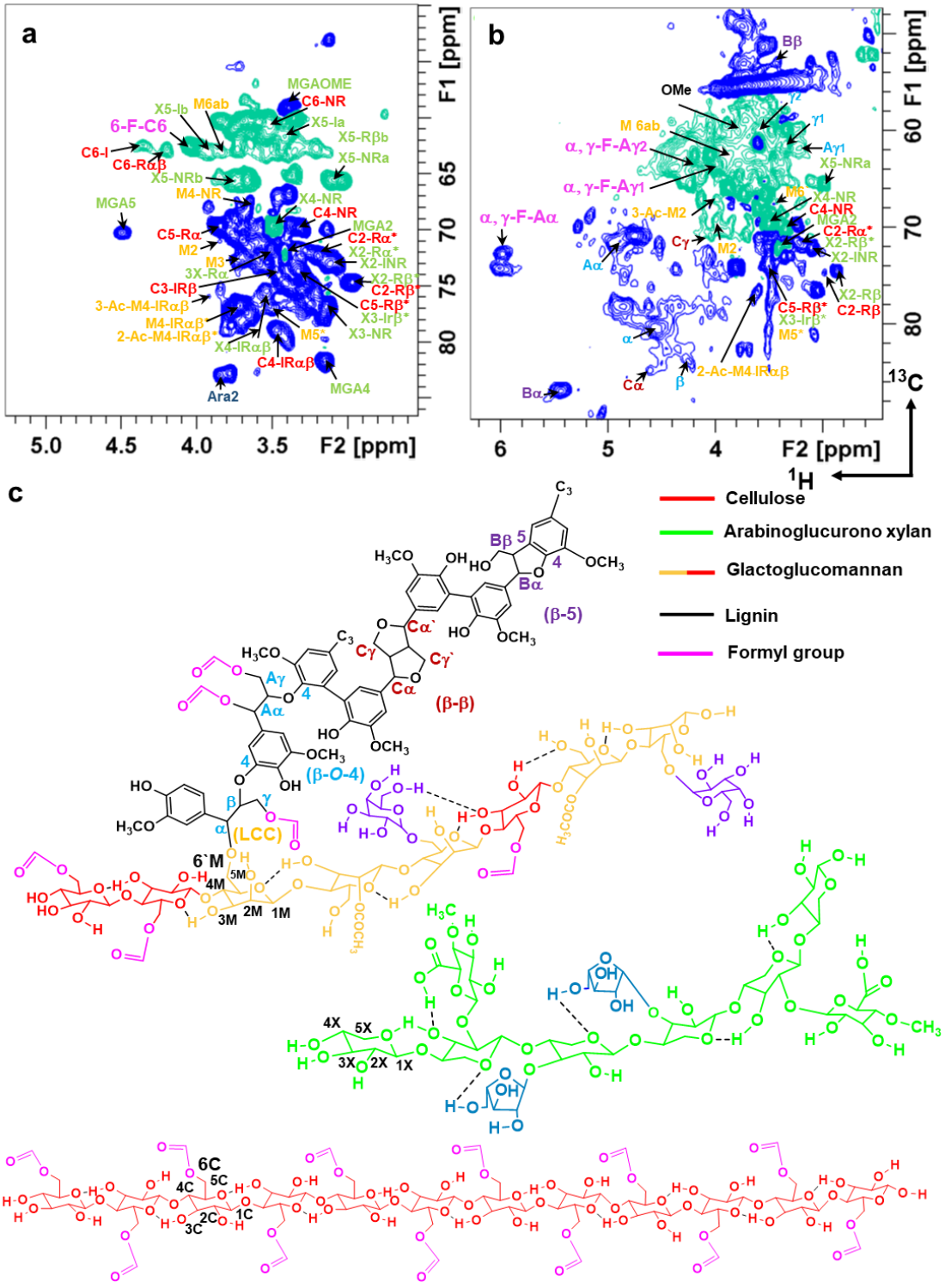

Figure S4: Aliphatic sidechain region of 2D ^{1}H-^{13}C HSQC spectra from the Japanese cedar heartwood film formed at 50 ℃. (a) ^{1}H-^{13}C HSQC spectrum of the polysaccharide-rich aqueous fraction. The signals from cellulose, arabinoglucuronoxylan, galactoglucomannan, and formylated compounds are shown in red, green, yellow/red, and pink, respectively. (b) ^{1}H-^{13}C

HSQC spectrum of the lignin-rich 2MeTHF fraction. The lignin linkages of β-*O*-4, β-β, β-5, and LCC are shown in blue, brown, purple, and yellow, respectively. The signal from Aα in the β-*O*-4 lignin unit differed from that of the benzyl ether linkage in LCC. Signals from galactoglucomannan are shown in yellow as M1 to M6/M6`. The signal assignment is shown in Tables S6, S7.

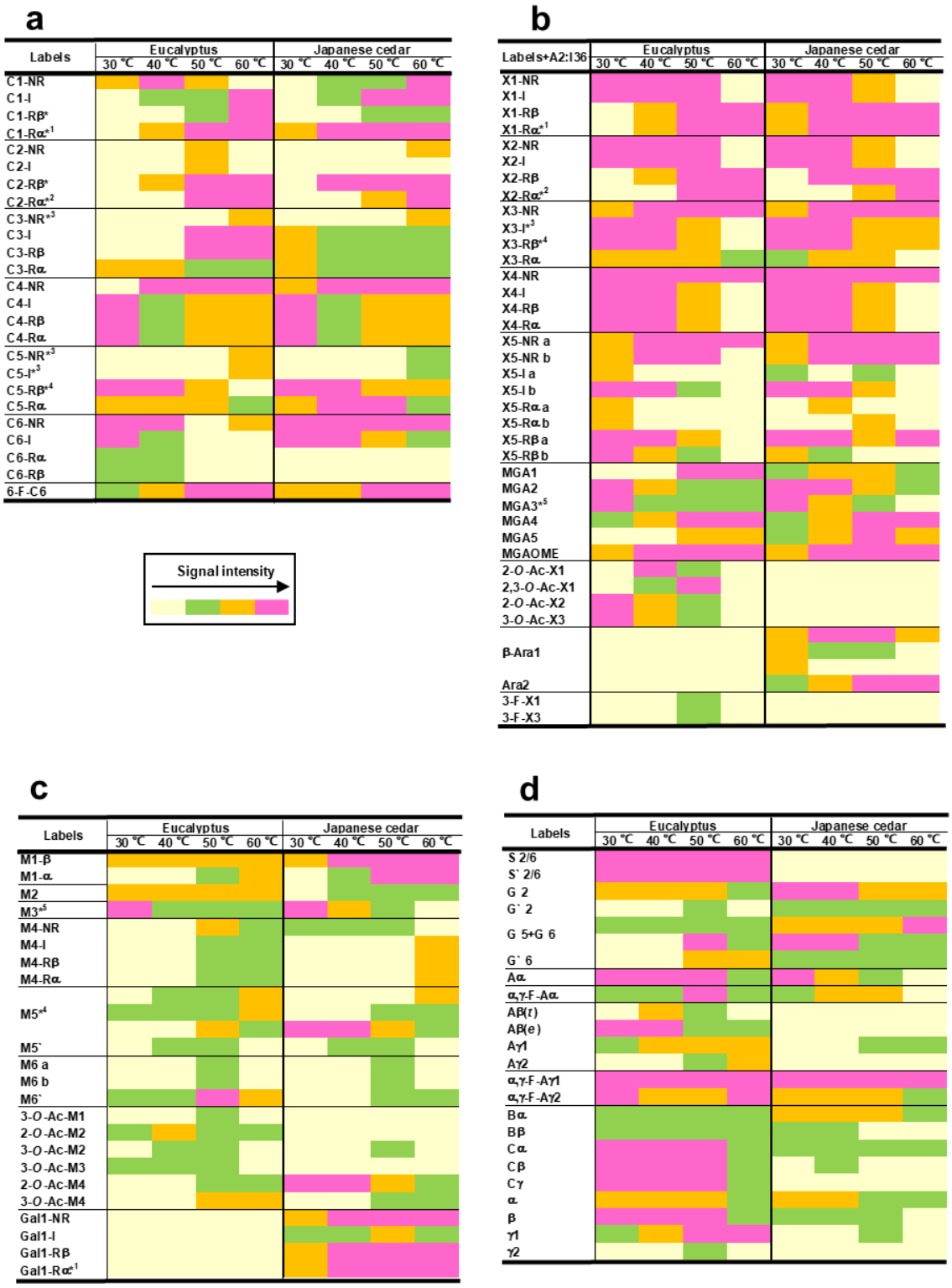

Figure S5: Comparison of signal intensity changes in cellulose, xylan, mannan, and lignin between Eucalyptus and Japanese cedar at 30 ℃–60 ℃ dissolving temperatures. a) Relative signal intensities of cellulose and formylated glucose residues. C-NR, cellulose nonreducing end unit; C-I, cellulose internal unit; C-Rα, α reducing end unit of cellulose; C-Rβ, β reducing

end unit of cellulose; 6-F-C, glucose residue formylated at 6 position in cellulose. (b) Relative signal intensities of xylan and formylated xylose residues. X-NR, xylan nonreducing end unit; X-I, xylan internal unit; X-Rα, α reducing end unit of xylan; X-Rβ, β reducing end unit of xylan; MGA, 4-*O*-methyl-α-D-glucuronic acid residue; Ac-X, acetylated xylose residue in xylan; Ara, arabinose residue. (c) Relative signal intensities of glucomannan. M-NR, nonreducing end unit in glucomannan; M-I, internal unit of glucomannan; M-Rα, α reducing end unit of glucomannan; M-Rβ, β reducing end unit of glucomannan; Ac-M, acetylated mannose residue in glucomannan; Gal-NR, galactose nonreducing end unit; Gal-I, galactose internal unit; Gal-Rα, galactose α reducing end unit; Gal-Rβ, galactose β reducing end unit. (d) Relative signal intensities of lignin. S, syringyl unit; S`, α-etherified syringyl unit; G, guaiacyl unit; G`, α-etherified guaiacyl unit; Aα, Aβ, Aγ, α, β and γ positions in β-*O*-4 unit; α, γ-F-A, β-*O*-4 unit formylated at α and/or γ positions; Bα, Bβ, α and β positions in β-5 unit; Cα, Cβ, Cγ, α, β and γ positions in β–β linkage. The chemical structures and positions are shown in Figure 7, and Scheme 1 and Figure S4. The signal assignment is tabulated in Tables S6, S7. The relative signal intensities were categorized into four groups: pale yellow, not detected; green, weak; orange, middle; pink, strong.

Table S6: Assignment of 2D ^{1}H-^{13}C HSQC NMR data for polysaccharides of Eucalyptus and Japanese cedar films. The names of lables are corresponding to those in Fugure S5.

Labels	HSQC δH (ppm)	HSQC δC (ppm)	Asingments	Wood Compositions
C1-NR	4.20	103.27	C_1-H_1 of β-D-glucopyranoside at non-reducing end	
C1-I	4.30	103.03	C_1-H_1 of β-D-glucopyranoside in internal	
C1-Rβ*	4.49	97.10	C_1-H_1 of β-D-glucopyranoside at reducing end	
C1-Rα*[1]	4.91	92.36	C_1-H_1 of α-D-glucopyranoside at reducing end	
C2-NR	2.91	72.89	C_2-H_2 of β-D-glucopyranoside at non-reducing end	
C2-I	2.98	72.80	C_2-H_2 of β-D-glucopyranoside in internal	
C2-Rβ*	2.97	74.64	C_2-H_2 of β-D-glucopyranoside at reducing end	Cellulose Glucomannan Galactoglucomannan
C2-Rα*[2]	3.20	72.16	C_2-H_2 of α-D-glucopyranoside at reducing end	
C3-NR*[3]	3.38	76.85	C_3-H_3 of β-D-glucopyranoside at non-reducing end	
C3-I	3.47	73.32	C_3-H_3 of β-D-glucopyranoside in internal	
C3-Rβ			C_3-H_3 of β-D-glucopyranoside at reducing end	
C3-Rα	3.65	71.54	C_3-H_3 of α-D-glucopyranoside at reducing end	
C4-NR	3.32	69.84	C_4-H_4 of β-D-glucopyranoside at non-reducing end	

C4-I			**C_4-H_4 of β-D-glucopyranoside in internal**	
C4-Rβ	**3.41**	**79.14**	**C_4-H_4 of β-D-glucopyranoside at reducing end**	
C4-Rα			**C_4-H_4 of α-D-glucopyranoside at reducing end**	
C5-NR*[3]	**3.38**	**76.85**	**C_5-H_5 of β-D-glucopyranoside at non-reducing end**	
C5-I*[3]			**C_5-H_5 of β-D-glucopyranoside in internal**	
C5-Rβ*[4]	**3.28**	**74.28**	**C_5-H_5 of β-D-glucopyranoside at reducing end**	
C5-Rα	**3.84**	**69.78**	**C_5-H_5 of α-D-glucopyranoside at reducing end**	
C6-NR	**3.38**	**61.10**	**C_6-H_6 of β-D-glucopyranoside at non-reducing end**	
C6-I	**3.51**	**60.64**	**C_6-H_6 of β-D-glucopyranoside in internal**	
C6-Rα	**3.69**	**60.29**	**C_6-H_6 of α-D-glucopyranoside at reducing end**	
C6-Rβ			**C_6-H_6 of β-D-glucopyranoside at reducing end**	
6-F-C6	**4.04**	**62.48**	**C_6-H_6 of formylated β-D-glucopyranoside at non-reducing end**	**Formylated cellulose**
X1-NR	**4.28**	**101.83**	**C_1-H_1 of β-D-xylopyranoside at non-reducing end**	**Glucurono xylan Arabinoglucurono Xylan**
X1-I			**C_1-H_1 of β-D-xylopyranoside in internal**	
X1-Rβ	**4.29**	**97.44**	**C_1-H_1 of β-D-xylopyranoside at reducing end**	
X1-Rα*[1]	**4.92**	**92.36**	**C_1-H_1 of α-D-xylopyranoside at reducing end**	

X2-NR	**3.11**	**72.57**	**C_2-H_2 of β-D-xylopyranoside at non-reducing end**
X2-I			**C_2-H_2 of β-D-xylopyranoside in internal**
X2-Rβ	**2.97**	**74.64**	**C_2-H_2 of β-D-xylopyranoside at reducing end**
X2-Rα*[2]	**3.20**	**72.16**	**C_2-H_2 of α-D-xylopyranoside at reducing end**
X3-NR	**3.15**	**76.65**	**C_3-H_3 of β-D-xylopyranoside at non-reducing end**
X3-I*[3]	**3.28**	**74.28**	**C_3-H_3 of β-D-xylopyranoside in internal**
X3-Rβ*[4]			**C_3-H_3 of β-D-xylopyranoside at reducing end**
X3-Rα	**3.51**	**71.59**	**C_3-H_3 of α-D-xylopyranoside at reducing end**
X4-NR	**3.49**	**69.57**	**C_4-H_4 of β-D-xylopyranoside at non-reducing end**
X4-I			**C_4-H_4 of β-D-xylopyranoside in internal**
X4-Rβ	**3.55**	**75.35**	**C_4-H_4 of β-D-xylopyranoside at reducing end**
X4-Rα			**C_4-H_4 of α-D-xylopyranoside at reducing end**
X5-NR a	**3.10**	**65.61**	**C_5-H_5 of β-D-xylopyranoside at non-reducing end a**
X5-NR b	**3.74**	**65.73**	**C_5-H_5 of β-D-xylopyranoside at non-reducing end b**
X5-I a	**3.35**	**63.04**	**C_5-H_5 of β-D-xylopyranoside in internal a**
X5-I b	**3.92**	**63.15**	**C_5-H_5 of β-D-xylopyranoside in internal b**
X5-Rα a	**3.52**	**58.12**	**C_5-H_5 of α-D-xylopyranoside at reducing end a**

X5-Rα b	**3.66**	**58.48**	**C_5-H_5 of α-D-xylopyranoside at reducing end b**
X5-Rβ a	**3.20**	**63.11**	**C_5-H_5 of β-D-xylopyranoside at reducing end a**
X5-Rβ b	**3.42**	**62.91**	**C_5-H_5 of β-D-xylopyranoside at reducing end b**
MGA1	**5.16**	**97.37**	**C_1-H_1 of 4-*O*-methyl-α-D-gluconic acid pyranoside at non-reducing end**
MGA2	**3.73**	**73.06**	**C_2-H_2 of 4-*O*-methyl-α-D-gluconic acid pyranoside at non-reducing end**
MGA3*[5]	**3.74**	**73.16**	**C_3-H_3 of 4-*O*-methyl-α-D-gluconic acid pyranoside at non-reducing end**
MGA4	**3.15**	**81.59**	**C_4-H_4 of 4-*O*-methyl-α-D-gluconic acid pyranoside at non-reducing end**
MGA5	**4.49**	**70.16**	**C_5-H_5 of 4-*O*-methyl-α-D-gluconic acid pyranoside at non-reducing end**
MGAOME	**3.38**	**59.02**	**C_{OMe}-H_{OMe} of 4-*O*-methyl-α-D-gluconic acid pyranoside acid at non-reducing end**
2-*O*-Ac-X1	**4.52**	**99.31**	**C_1-H_1 of 2-*O*-acetyl-β-D-xylopyranoside**
2,3-*O*-Ac-X1	**4.62**	**101.06**	**C_1-H_1 of 2,3-*O*-acethyl-β-D-xylopyranoside**
2-*O*-Ac-X2	**4.56**	**73.28**	**C_2-H_2 of 2-*O*-acethyl-β-D-xylopyranoside**
3-*O*-Ac-X3	**4.87**	**74.76**	**C_3-H_3 of 3-*O*-acethyl-β-D-xylopyranoside**
β-Ara1	**5.00**	**101.77**	**C_1-H_1 of β-D-arabinofranoside**
	5.08	**100.45**	**C_1-H_1 of β-D-arabinofranoside**

	5.17	**100.02**	**C_1-H_1 of β-D-arabinofranoside**	
Ara2	**3.85**	**82.80**	**C_2-H_2 of β-D-arabinofranoside**	
M1-β	**4.48**	**101.50**	**C_1-H_1 of β-D-mannopyranoside at reducing end**	
M1-α	**4.97**	**93.73**	**C_1-H_1 of α-D-mannopyranoside at reducing end**	
M2	**3.85**	**71.17**	**C_2-H_2 of β-D-mannopyranoside**	
M3*[5]	**3.74**	**72.53**	**C_3-H_3 of β-D-mannopyranoside**	
M4-NR	**3.67**	**67.79**	**C_4-H_4 of β-D-mannopyranoside at non-reducing end**	
M4-I			**C_4-H_4 of β-D-mannopyranoside in internal**	
M4-Rβ	**3.76**	**76.55**	**C_4-H_4 of β-D-mannopyranoside at reducing end**	**Glucomannan Galactoglucomannan LCC**
M4-Rα			**C_4-H_4 of α-D-mannopyranoside at reducing end**	
	3.38	**76.85**		
M5*[4]	**3.51**	**76.63**	**C_5-H_5 of β-D-mannopyranoside**	
	3.70	**76.55**		
M5`	**3.69**	**69.26**	**LCC $C_{5`}$-$H_{5`}$ of β-D-xylopyranoside**	
M6 a			**C_6-H_6 of β-D-mannopyranoside a**	
	3.84	**62.66**		
M6 b			**C_6-H_6 of β-D-mannopyranoside b**	

M6`	**3.49**	**67.83**	**LCC $C_{6`}$-$H_{6`}$ of β-D-xylopyranoside**
3-*O*-Ac-M1	**4.79**	**98.87**	**C_1-H_1 of 3-*O*-acetyl-β-D-mannopyranoside**
2-*O*-Ac-M2	**4.98**	**72.66**	**C_2-H_2 of 2-*O*-acetyl-β-D-mannopyranoside**
3-*O*-Ac-M2	**3.78**	**68.96**	**C_2-H_2 of 3-*O*-acetyl-β-D-mannopyranoside**
3-*O*-Ac-M3	**4.78**	**77.25**	**C_3-H_3 of 3-*O*-acetyl-β-D-mannopyranoside**
2-*O*-Ac-M4	**3.70**	**76.55**	**C_4-H_4 of 2-*O*-acetyl-β-D-mannopyranoside**
3-*O*-Ac-M4	**3.92**	**75.54**	**C_4-H_4 of 3-*O*-acetyl-β-D-mannopyranoside**
Gal1-NR	**4.91**	**92.36**	**C_1-H_1 of β-D-galactopyranoside at non-reducing end**
Gal1-I	**4.32**	**105.16**	**C_1-H_1 of β-D-galactopyranoside in internal**
Gal1-Rβ	**4.28**	**97.49**	**C_1-H_1 of β-D-galactopyranoside at reducing end**
Gal1-Rα*[1]	**4.91**	**92.36**	**C_1-H_1 of α-D-galactopyranoside at reducing end**

Table S7: Assignment of 2D ^{1}H-^{13}C HSQC NMR data for lignin and LCC of Eucalyptus and Japanese cedar films. The names of lables are corresponding to those in Fugure S5.

Labels	HSQC		Asingments	Wood Compositions
	δH (ppm)	δC (ppm)		
S 2/6	6.65	103.50	C_2-H_2/C_6-H_6 of syringyl units	
S` 2/6	7.30	106.30	C_2-H_2/C_6-H_6 of syringyl units with α linkage	
G 2	6.98	110.84	C_2-H_2 of guaiacyl units	
G` 2	7.47	111.66	C_2-H_2/C_6-H_6 of guaiacyl units with α linkage	Aromatic units
G 5+G 6	6.92	115.31	C_5-H_5+C_6-H_6 of guaiacyl units	
	6.78	118.90		
G` 6	7.34	124.06	C_6-H_6 of guaiacyl units with α linkage	
Aα	4.86	71.51	C_a-H_a of β-*O*-4 linkages	Linkages of ligin and LCC
α,γ-F-Aα	6.02	73.69	$C_α$-$H_α$ of β-*O*-4 formylated linkages	Formylated β-*O*-4 of lignin
Aβ(*t*)	4.01	86.62	$C_β$-$H_β$ of β-*O*-4 linkages linked to a syringyl unit (*threo* form)	Linkages of ligin and LCC
Aβ(*e*)	4.10	85.93	$C_β$-$H_β$ of β-*O*-4 linkages linked to a syringyl unit (*erythro* form)	
Aγ1	3.21	62.00	$C_{γ1}$-$H_{γ1}$ of β-*O*-4 linkages	
Aγ2	3.53	60.69	$C_{γ2}$-$H_{γ2}$ of β-*O*-4 linkages	

α,γ-F-Aγ1	3.92	63.27	$C_{\gamma1}$-$H_{\gamma1}$ of formylated β-*O*-4 linkages	Formylated β-*O*-4 of lignin
α,γ-F-Aγ2	4.18	63.07	$C_{\gamma2}$-$H_{\gamma2}$ of formylated β-*O*-4 linkages	
Bα	5.44	86.82	C_{α}-H_{α} of β-5 linkages	
Bβ	3.49	53.45	C_{β}-H_{β} of β-5 linkages	
Cα	4.65	84.89	C_{α}-H_{a} of β-β linkages	
Cβ	3.05	53.57	C_{β}-H_{β} of β-β linkages	
Cγ	41.17	71.14	C_{γ}-H_{γ} of β-β linkages	Linkages of lignin
α	4.55	80.20	LCC C_{α}-H_{α} of β-*O*-4 linkages	
β	4.30	83.19	LCC C_{β}-H_{β} of β-*O*-4 linkages	
γ1	3.34	61.62	LCC $C_{\gamma1}$-$H_{\gamma1}$ of β-*O*-4 linkages	
γ2	3.61	60.15	LCC $C_{\gamma2}$-$H_{\gamma2}$ of β-*O*-4 linkages	